INTERNATIONAL JOURNAL OF Electroactive Materials

Int. J. Electroactive Mater. **6 (2018) 14-20**
www.electroactmater.com

RECEIVED
05 June 2018

REVISED
24 June 2018

ACCEPTED FOR PUBLICATION
15 July 2018

PUBLISHED
06 Aug 2018

Study of DC conductivity in nanostructured ceramics of $NiMn_2O_4$ pure and doped with Cu and Zn

V.A. Soares, A.F. Santos, D.M. S. Ribeiro, M.S. Silva *

Federal Institute of Education, Science and Technology of Sertão Pernambucano, Salgueiro, Pernambuco, 56000-000, Brazil
E-mail: ssiilva990@hotmail.com*

ABSTRACT: In this paper we present the structural, DC electrical characterization of ceramics based on nickel manganite ($NiMn_2O_4$, NMO) pure and doped with 5 mole % of Cu^{2+}, and Zn^{2+} produced by the sol-gel method. The ceramic bodies of nickel manganite were sintered at a temperature of 1000 °C during 3 h. The structural characterization was based on the techniques of the scanning electron microscopy (SEM), X-ray diffraction (XRD). The resistivity was studied using temperature dependent resistance measurements (TDR). This work aims to produce and characterize nickel manganite ceramics obtained by nanopowders with a single cubic phase synthesized using the sol-gel method. It will study the influence on the microstructure and the electrical conductivity of the addition of transition metals such as Zn^{2+} and Cu^{2+}, a novelty for this system. The crystallite size and particle size, respectively obtained by XRD and SEM, were of around 50 nm and 0.7 µm. The pure samples showed NTCR behavior, but the addition of the dopant allows reducing the activation energy by making them semiconductor, resulting in many different resistivity values at room temperature.
Keywords: nickel manganite, ceramics, sol–gel method, NTCR, spinel

1. Introduction

Many researchers have extensively studied nano and micro-structures materials containing transition metals being. For example, Ti, Ni, Zn, Mn, Cu, Pb compounds, something of the most studied [1-7]. There is much work in the literature on various compounds produced under forms of monocrystals, polycrystals, ceramics, films, polymers, glass, etc., starting from different synthesis routes [2, 3]. These works, in general, seek to achieve a deeper understanding of the materials properties, which can result in innovative applications. Nickel manganite is a promising material having a partially inverse spinel type structure and is often used in the production of temperature sensors due to the negative temperature coefficient (NTC). A uniform exponential decrease of resistivity with increasing temperature, where the growth of the conductivity is attributed to the transport property of the charge, which for semiconductors is characterized by tetrahedral-bonded, is elucidated by the extended-state model [4, 5].

NMO is a binary oxide that meets various technological applications, for example, temperature protection device, humidity sensor [6], catalytic systems that act in the decomposition process of ozone, etc. [7, 8]. In addition, nickel and manganese oxides can be considered as ideal candidates for obtaining electrode materials because of their abundance, low-cost and low toxicity to the environment [6, 7]. The spinel-like structure consists of cations filling the tetrahedral, which will be referred to as site A, and octahedral site, to which we will assign the denomination of site B, in the FCC sub-lattice of oxygen [9, 10]. The nickel cations preferentially occupy the octahedral B-sites over the tetrahedral A-sites of the cubic close-packed oxygen sub-lattice (an inverse spinel) [11].

The present debate in the literature tries to understand the influence of the synthesis route and contaminants of the microstructure on the electro-optical properties of the material [12, 13]. Thus, this article aims to present a study of the electrical and structural properties of $NiMn_2O_4$ ceramics, pure and doped with zinc or copper and synthesized using the sol-gel method [14, 15]. This method was chosen with the intention of obtain nanostructured powders for the production of MNO ceramics. The characterizations by XRD, SEM and temperature-dependent resistance (TDR) measurements.

2. Experimental

The sol-gel method was chosen as the synthesis route, aiming to obtain nanocrystals of NMO. Initially, a 2M solution of glycine ($C_2H_5NO_2$) was used as chelating agent and 3 g of citric acid ($C_6H_8O_7$) as complexing agent. This mixture was added to a solution containing the appropriate mixture of solid precursors Ni $(NO_3)_2{\cdot}6(H_2O)$ and ($MnCl_2$). To obtain the doped samples of nickel manganite, the appropriate proportions (5 mole % of the divalent Cu^{2+} and Zn^{2+}) of Copper (II) nitrate (Cu $(NO_3)_2$, Zinc nitrate hexahydrate (Zn $(NO_3)_2{\cdot}6(H_2O)$ were added and stirred until complete dissolution. This solution was heated at 100 °C for 24

hours to remove excess water and, consequently, obtain a viscous solid gel (xerogel) [16]. Finally, the xerogel was subjected to a heat treatment with a temperature of 700 ºC for one hour.

To obtain green ceramics, the powders produced were added to at 10 % binder solution (PVA) and pressed uniaxial under pressure of 100 kgf/cm^2, resulting in cylindrical bodies which were subsequently sintered at 1000 ºC for 3 hours, resulting in nickel manganite-based ceramics. A representation of the synthesis pathway by the sol-gel method is shown in **Fig. 1**.

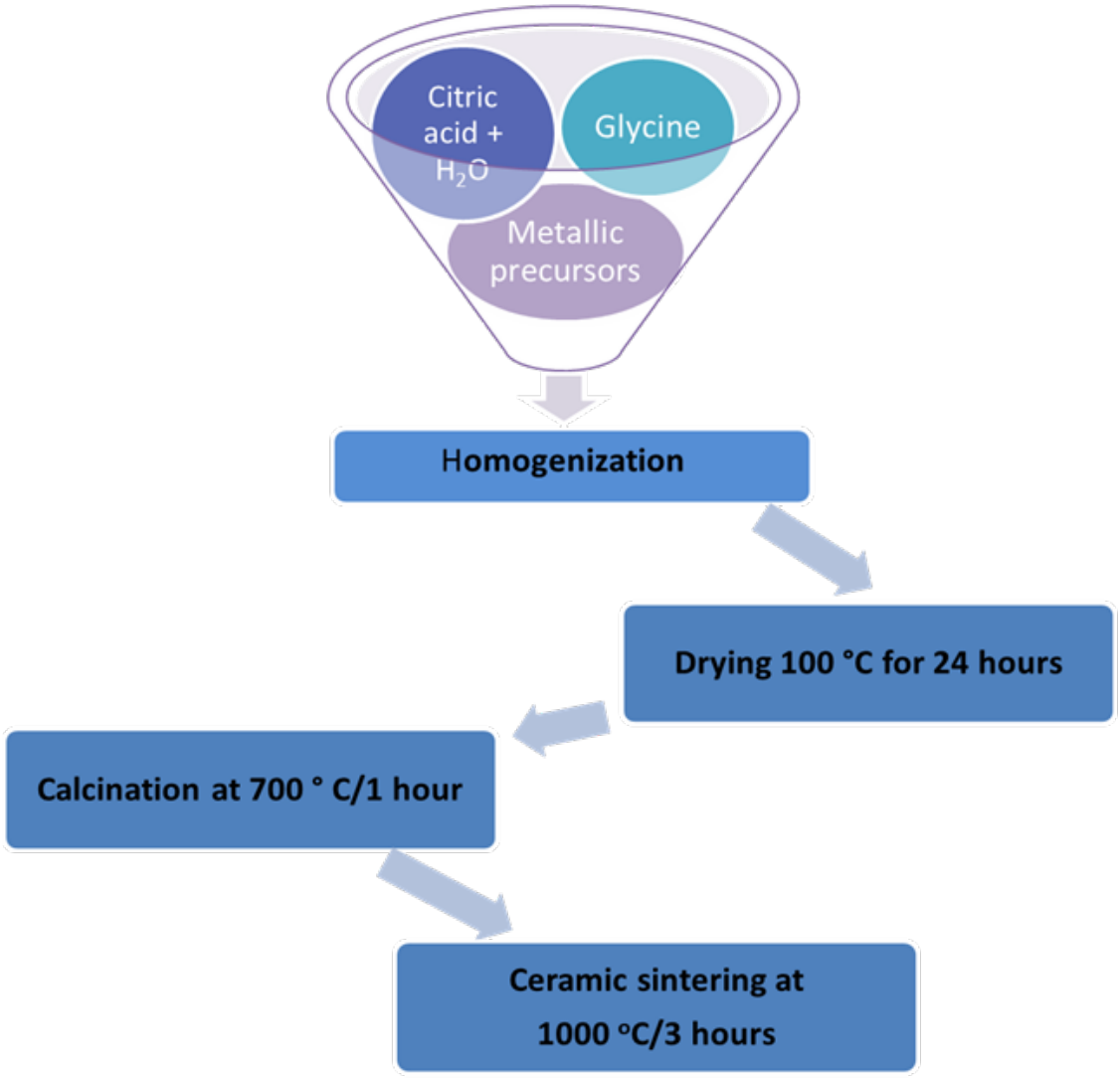

Figure 1. Summary flowchart of the sol-gel method

A scanning electron microscope (SEM) (JSM-6510 LV model) was used to study the surface of the samples without any polishing or chemical treatment. A Bruker diffractometer, operating under 40 KV and 40 mA, performed X-ray diffraction (XRD) measurements in the range of 2θ between 20 and 70º in continuous mode at a scanning speed of 0.04 º/min. With the aid of the Rex program, adjustments were made to the Rietveld refinement for all samples. [17, 18]. In the ceramics bodies, metal electrodes made with colloidal silver paint were produced. The temperature-dependent resistivity curve was obtained with geometric parameters of the sample and DC electrical conductivity measurements carried out at a temperature range of 30 to 200 ºC with the help of a precise digital multimeter (Hikari 2090 HM) in the cooling cycle.

3. Results and discussion

Table 1 shows the nomenclature that will be used in this work as well as the relative densities obtained for each sample. It is possible to observe that the copper-doped sample had a lower density than the others. Zinc doping, in turn, did not interfere in densification compared to the pure sample.

Fig. 2a presents the XRD patterns obtained for each sample sintered at 1000 °C/3 h exhibited single phase. This result indicates that the sol-gel method can be considered as an alternative in the production of $NiMn_2O_4$ ceramics.

In **Fig. 2a**, the peaks related to the families of crystalline planes (220), (311), (222), (400), (331), (422) and (511) were indexed. These peaks correspond to the spinel phase, belonging to the spatial group (Fd- 3m). The average crystallite sizes, D, were estimated by the Scherrer formula presented by [19, 20]. The pure sample (NMO) presented a crystallite size of approximately 41.60 nm, while the doped samples (NMO: Cu and NMO: Zn), showed crystallite size from approximately 53.5 and 69.0 nm. The structural parameters of the samples were obtained from the Reitveld. The background is estimated by a polynomial function of degree 5 and peak diffraction profile was adjusted by the Pseudo-Voigt function, which is the convolution of Gaussian and Lorentzian function.

Fig. 2b shows a typical Rietveld fit for the MNO samples. The occupation factors obtained indicate that an effect of the addition of dopants was an increase of Mn ions at site A. Consequently a reduction of the proportion of Ni ions at site A. From the adjustments it was possible to obtain data such as crystallite size and lattice parameters shown in **Table 1**.

The samples NMO, NMO: Cu and NMO: Zn, (**Fig. 3**), present average grain size of 0.7, 1.5 and 1.2 µm, respectively. This behavior was expected because the accommodation of the dopants in the net increases the possibility of the Ni ions to settle in the B site of the structure, corroborating with the Rietveld refinement, contributing to mass diffusion and thus increasing the crystallization rate of solid phase [16]. So, it is possible to state that the samples have a grain size of the order of micrometers. These grains are formed by crystallographic units (crystallites size obtained by Rietveld refinement), with dimensions of the order of nanometers.

Table 1: Nomenclature and density of nickel manganite oxide (NMO) samples, sintered at 1000 °C/3 hours.

Nomenclature	Sample	Relative Density (%)	Crystallite size (nm)	Lattice parameters
NMO	(Pure)	(90 ± 1)	41.6	8.393(9)
NMO:Cu	(Cu at 5 mole %)	(84 ± 2)	69.0	8.394(0)
NMO:Zn	(Zn at 5 mole %)	(90 ± 2)	53.5	8.394(3)

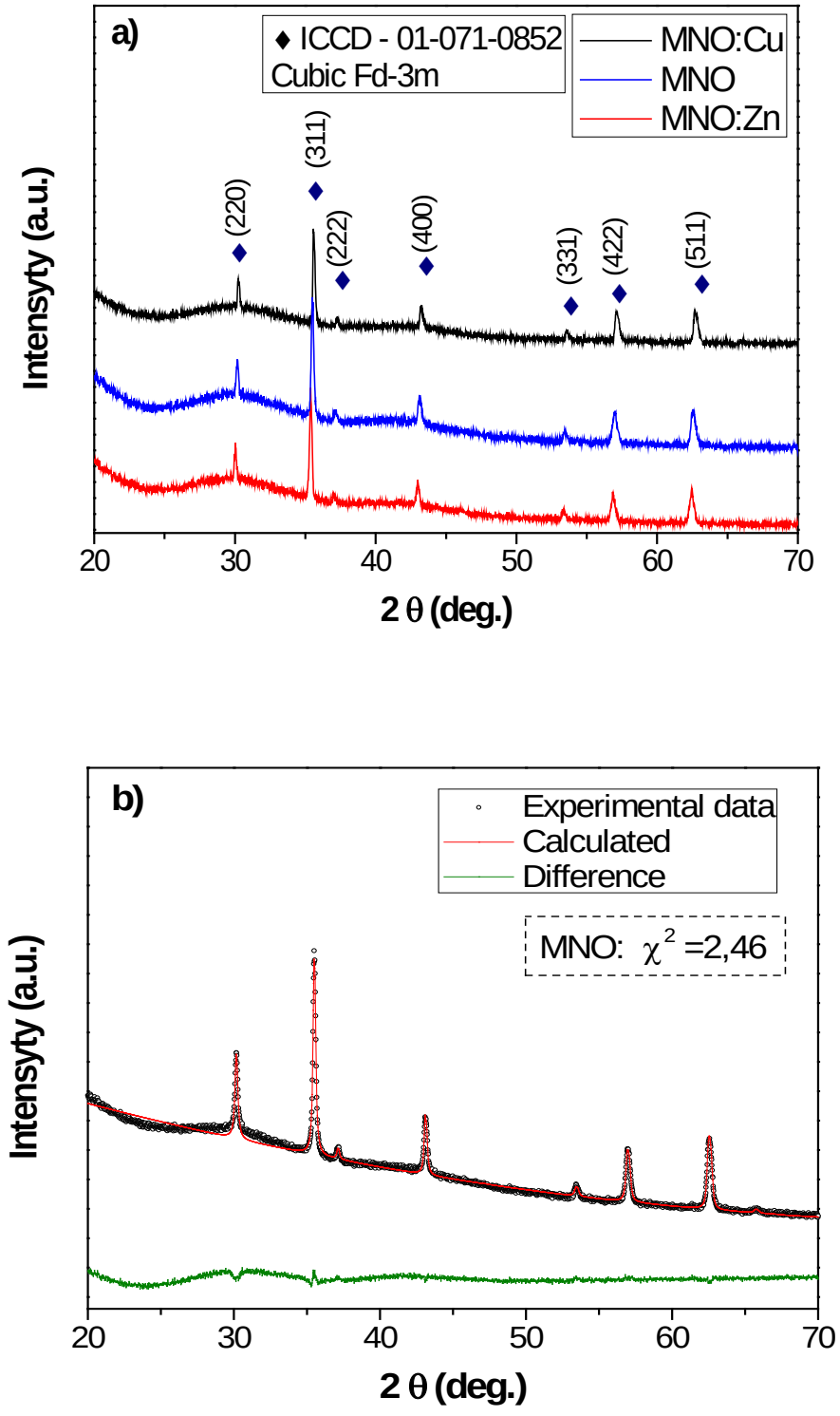

Figure 2. (a) XRD patterns of the $NiMn_2O_4$ ceramics and (b) graphic example of Rietveld fit.

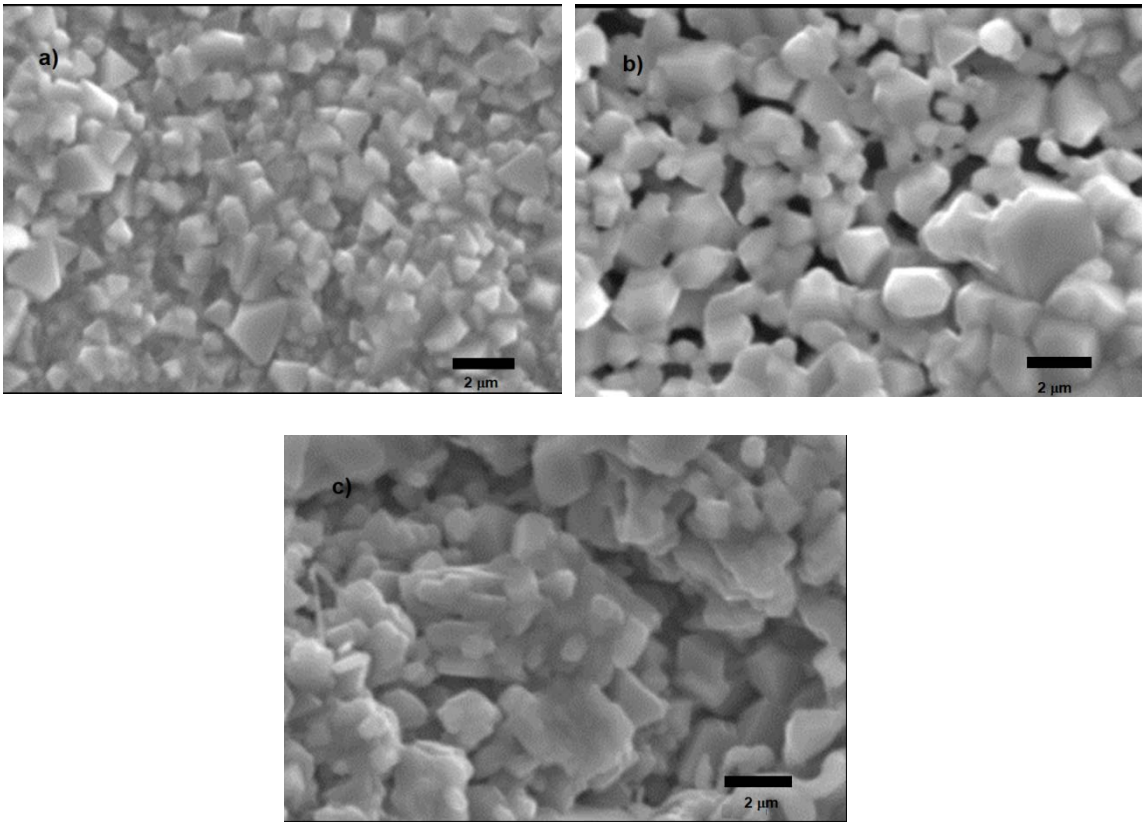

Figure 3. SEM images of ceramic $NiMn_2O_4$ (scale 2 µm). (a) NMO, (b) NMO: Cu, and (c) NMO: Zn

Fig. 4 shows the electrical resistivity measures in the nickel manganite ceramics. The resistivity of NMO and NMO: Zn decays exponentially as a function of the temperature increase. The resistivity (ρ) characteristics were measured at different temperatures in the range of (30-200 ºC). **Fig. 4** shows that the sample (NMO: Cu) has a decrease of the activation energy, exhibiting a typical semi conductivity behavior. Starting from equation (1) it is possible to obtain the activation energy (E_a) using the resistivity data as a function of temperature:

$$\boldsymbol{\rho = \rho_0 e^{E_a/KT}} \quad (1)$$

In equation (1) ρ_0 is a constant, k is the Boltzmann constant, T is the temperature in Kelvin, E_a is the activation energy for electrical conduction obtained through the angular coefficient fit of the data of ln(ρ) as a function of 1000/T [21, 22]. Thus, it is possible to observe that Cu doping results in a major contribution on the conductivity of MNO samples, as shown in **Fig. 4**. These results reveal that doping ion is a parameter that can be adjusted to change the conductivity of the system or even obtain NTC thermistors with different characteristics [23].

According to **Fig. 4**, the insertion of the dopants implies a decrease in the activation energy that is directly proportional to the room temperature resistivity [21]. This behavior can be explained as due to wedded changes in the lattice that induces a greater amount of Ni ions in the B site of the AB_2O_4 structure; the spinel structure rich in antisite defects approach metallic-like behavior [22].

In general, a normal spinel-type structure presents divalent cations (A) that occupy tetrahedral and trivalent cations (B) as well as octahedral sites. The insertion of Zn^{2+} and Cu^{2+} induced the crystal structure for one type of mixed spinel structure; a small portion of atoms A and B occupy both octahedral and tetrahedral sites. In this way the structure $NiMn_2O_4$ becomes of the type $(A_{1-x}Mn_x)(A_xMn_{2-x})O_4$, which A = (Ni, Zn or Cu), implying a higher concentration of Mn^{4+} ions, consequently enabling hopping conduction between Mn^{3+} and Mn^{4+} ions present in the octahedral sites, thus causing increased conductivity [24]. That is, the entry of the divalent cations (Cu, Zn, Ni) at site B must result in a corresponding proportion of Mn^{3+} cations on B-sites disproportionate to Mn^{2+} and Mn^{4+}, and the Mn^{2+} cations move to the A-sites to compensate Ni^{2+} vacancies. The Mn mixed valence and random crystal field fluctuations may lead to the formation of localized small polarons which can perform hopping if thermally activated [22-24].

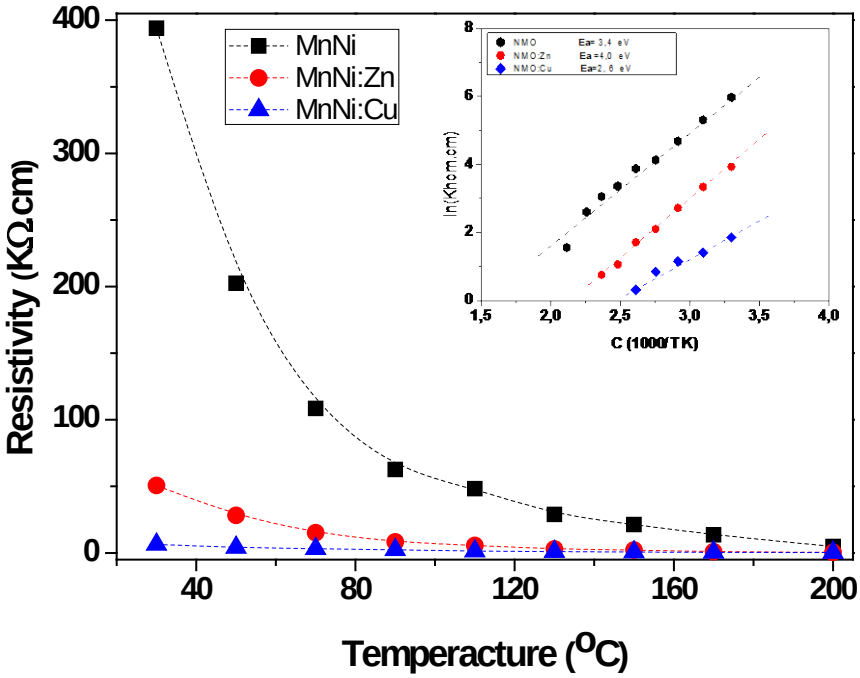

Figure 4. Resistivity curves as a function of temperature of NMO ceramics sintered at 1000 °C for 3 h

4. Conclusion

In summary, the sol-gel method was used successfully as a synthesis route for nanostructured $NiMn_2O_4$ ceramics. XRD results showed all the samples (NMO, NMO: Cu, NMO: Zn) consist of a single phase belonging to the space group (Fd-3m). The analysis of the images obtained by electron microscopy showed that the average grain size ranged from 0.7 to 1.5 µm, as a function of the different dopants.

It was observed that the copper-doped sample had higher porosity, higher conductivity at room temperature and lower activation energy when compared to the other samples. Doping significantly altered the electrical parameters. In this work, it was observed that the room temperature resistivity obtained were approximately ($4{\cdot}10^2$, $5{\cdot}10^1$ and $7{\cdot}10^0$) KΩ·cm for the NMO, NMO: Zn and NMO: Cu ceramics, respectively. Similar effects of microstructural factors, grain size and porosity of the ceramics NMO and NMO: Zn were obtained. Therefore, it is possible to confirm that the changes caused by dopants in the electronic configuration of the system and in the proportion of the accommodation of Mn ions in sites A and B are the main factors that result in the alteration of the electrical properties of the nanostructured NMO.

Acknowledgement

This work has been partially supported by a research grant from IF-Sertão Pernambucano.

References

1. P. Geng, S. Zheng, H. Tang, R. Zhu, L. Zhang, S. Cao, H. Xue and H. Pang, Transition Metal Sulfides Based on Graphene for Electrochemical Energy Storage, *Adv. Energy Mater.* 1703259; 2018, 1–26.
2. Y. Li, Y. Xu, W. Yang, W. Shen, H. Xue and H. Pang, MOF-derived Metal Oxide Composites for Advanced Electrochemical Energy Storage, *Small*, 1704435 14 (2018), 1–24.
3. H. Pang, X. Li, Q. Zhao, H. Xue, W. Lai, Z. Hu, W. Huang, One-pot synthesis of heterogeneous Co_3O_4-nanocube/$Co(OH)_2$-nanosheet hybrids for high-performance flexible asymmetric all-solid-state super capacitors. *Nano Energy*, 35 (2017) 138–145.
4. M. Zhang, S. Guo, L. Zheng, G. Zhang, Z. Hao, L. Kang, Z-H. Liu, Preparation of $NiMn_2O_4$ with large specific surface area from an epoxide-driven sol-gel process and its capacitance. *Electrochimica Acta.* 87 (2013) 546–553.

5. J. M. A. Almeida, C. T. Meneses, A. S. de Menezes, R. F. Jardim, J. M. Sasaki, Synthesis and characterization of $NiMn_2O_4$ nanoparticles using gelatin as organic precursor. *Journal of Magnetism and Magnetic Materials* 320 (2008) 304–307.
6. Y. Gawli, S. Badadhe, A. Basu, D. Guin, M. V. Shelke, S. Ogale, Evaluation of n-type ternary metal oxide $NiMn_2O_4$ nanomaterial for humidity sensing. *Sensors and Actuators B* 191 (2014) 837–843.
7. X. Tang, H. Li, Z-H. Liu, Z. Yang, Z. Wang, Preparation and capacitive property of manganese oxide nanobelt bundles with birnessite-type structure. *Journal of Power Sources* 196 (2011) 855–859.
8. T. Larbi, A. Amara, B. Ouni, A. Inoubli, M. Karyaoui, A. Yumak, F. Saadallah, K. Boubaker, M. Amlouk, Physical investigations on $NiMn_2O_4$ sprayed magnetic spinel for sensitivity applications. *Journal of Magnetism and Magnetic Materials* 387 (2015) 139–146.
9. S. M. Savić, M. Tadić, Z. Jagličić, K. Vojisavljević, L. Mancicd, G. Branković, Structural, electrical and magnetic properties of nickel manganite obtained by a complex polymerization method. *Ceramics International* 40 (2014) 15515.
10. J-R. Huang, H. Hsu, C. Cheng, Strongly reduced band gap in $NiMn_2O_4$ due to cation exchange. *Journal of Magnetism and Magnetic Materials* 358 (2014) 149–152.
11. H. Pang, J. Deng, S. Wang, S. Li, J. Du, J. Chen, J. Zhang, Facile synthesis of porous nickel manganite materials and their morphology effect on electrochemical properties. *RSC Advances.* 14, (2012) 5930–5934.
12. S. Mhin, H. Han, K. M. Kim, J. Lim, D. Kim, J. Lee, H. J. Ryu, Synthesis of $(Ni,Mn,Co)O_4$ nanopowder with single cubic spinel phase via combustion method. *Ceramics International* 42(2016) 12, 13654–13658.
13. G. Ashcroft, I. Terry, R. Gover, Study of the preparation conditions for $NiMn_2O_4$ grown from hydroxide precursors. *Journal of the European Ceramic Society* 26 (2006) 901–908.
14. N. S. Ferreira, R. S. Angélica, V. B. Marques, C. C. O. de Lima, M. S. Silva, Cassava-starch-assisted sol–gel synthesis of CeO_2 nanoparticles. *Materials Letteres* 165 (2016) 139–142.
15. M. Kotobuki, Fabrication of Thin $LiMn_2O_4$ Electrode on the $Li_{1.5}Al_{0.5}Ge_{1.5}$ $(PO_4)_3$ Solid Electrolyte by a Sol-Gel Method. *International Journal of Electroactive Materials* 1 (2013) 50–54.
16. J. C. A. Menezes, N. S. Ferreira, L. G. Abraçado, M. A. Macêdo, Synthesis and Characterization of Nickel Nanoparticles Prepared Using the Aquolif Approach. *Journal of Nanoscience and Nanotechnology*, 14, 8, (2014) 5903–5910(8).
17. M. Bortolotti, L. Lutterotti and I. Lonardelli, ReX: A computer program for structural analysis using powder diffraction data, *Journal of Applied Crystallography* 42, (2009) 538–539.
18. B. D. Cullity, S. R. Stock, *Elements of X-Ray Diffraction*. (Prentice-Hall, 3rd Ed. New Jersey, 2001).
19. N. S. Ferreira, A. C. B. Oliveira, G. V. S. Mota, A. C. Cunha, M. A. Silva, X-Ray Peak Broadening and Raman Spectroscopy Studies of $Ce_{0.08}Fe_{0.02}O_{2-\delta}$ Nanoparticles Prepared by a Sol-Gel-Based Method. *Materials Science Forum* 881 (2016) 491-496.
20. E. Carvalho, V. Soares, C. A. Leães, G. E. Paiva, R. S. Silva, M. S. Silva, Radioluminescence study of calcium tungstate crystalline powders and ceramics. *International Journal of Applied Ceramic Technology* 14 (2017) 1-4.
21. A. C. B. Oliveira, D. M. S. Ribeiro, C. G. P. Moraes, R. S. Silva, N. S. Ferreira, M. S. Silva, Synthesis and Characterization of Nickel Manganite Ceramics by Polymeric Precursors Method. *Materials Science Forum* 881(2016) 123-127.
22. R. Schmidt, A. Basu, A. W. Brinkman, Small polaron hopping in spinel manganates *Physical Review B* 72 (2005) 115101.
23. A. L. Dzubak, C. Mitra, M. Chance, S. Kuhn, G. E. Jellison, A. S. Sefat, J. T. Krogel, F. A. Reboredo, $MnNiO_3$ revisited with modern theoretical and experimental methods. *The Journal of Chemical Physics* 147, (2017) 174703.
24. S. Lee, D. Lee, K. Kim, M. Park, Cation Distribution in Ni-Mn-O Spinel System for the Application of IR Sensors. *Procedia Engineering* 168 (2016) 1279 – 1282.